

# Fourier Analysis of Alternating Current Polarography: Amplitude and Phase of Fundamental and Second Harmonic AC Polarographic Waves

Hiroyuki KOJIMA and Shizuo FUJIWARA

Department of Chemistry, Faculty of Science, The University of Tokyo, Hongo

(Received February 19, 1971)

The Fourier analysis of the instantaneous AC polarographic current was performed with a computer *on-lined* to a potentiostat. From the Fourier spectra, the amplitudes and phase angles of both the fundamental and the second harmonic AC polarographic waves were obtained. In the Cd(II) system, the current amplitude DC potential curves and phase angle-DC potential curves for the fundamental and the second harmonic AC polarographic waves were compared with the theoretical curves. The method is applicable to the accurate analysis of electrode reaction kinetics.

Alternating current (AC) polarography has been found to be useful in studying electrode reaction kinetics, and various instrumental and theoretical approaches have been attempted. The phase angle of the fundamental harmonic AC wave and the intensity of higher order harmonic AC waves were measured and analyzed theoretically by Smith and his coworkers,<sup>1-7)</sup> who employed a potentiostat with a phase-sensitive detector and tuned amplifiers.

In the present work, it is shown that Fourier analysis of instantaneous AC polarographic waves gives the phase angle and amplitude of fundamental and second harmonic AC polarographic waves. In general, AC polarographic waves can be expressed in the following form.

$$I = I_1 \sin(\omega t + \varphi_1) + I_2 \sin(2\omega t + \varphi_2) + \dots \quad (1)$$

where  $\omega$  is the angular frequency of an applied AC potential,  $I$  is the total alternating current,  $I_1$  ( $I_2$ ) and  $\varphi_1$  ( $\varphi_2$ ) are the amplitude and phase angle of the fundamental (second) harmonic AC polarographic wave, respectively. The Fourier transforms of Eq. (1) are

$$I_k \cos \varphi_k = \frac{2}{T} \int_0^T I \sin k\omega t \, dt \quad (2)$$

$$I_k \sin \varphi_k = \frac{2}{T} \int_0^T I \cos k\omega t \, dt \quad (3)$$

$$k = 1, 2, \dots,$$

where  $T$  is the period of original data. Equations (2) and (3) show that both the amplitude and phase angle of the fundamental and the second harmonic AC polarographic waves can be obtained by the Fourier transformation.

In this paper, an instrumentation for the Fourier transformation is presented and the feasibility of this method for the measurement of faradaic currents is discussed.

## Experimental

**Outline of the Procedure.** Figure 1 shows a block-diagram of the apparatus, which is a modified version of a digital polarograph used to analyze fluctuations of  $i$ - $t$  curves.<sup>8)</sup> It is composed of a potentiostat, a computer,<sup>9)</sup> a synchroscope<sup>10)</sup> and their supporting equipments. A sinusoidal alternating potential with small amplitude is superposed on the direct current potential which is applied to the electrode. Using the dropping mercury electrode, the polarographic current on which the AC wave is superposed is sampled during the single drop life, and is stored in the computer which is *on-lined* to the potentiostat. The Fourier transformation is performed after the DC component of the polarographic current is eliminated by shifting the zero level. Calculated Fourier spectra are recorded on a chart paper in bar-graph style.

**Potentiostat.** The potentiostat is constructed mainly from solid-state operational amplifiers. A three-electrode cell is used with the voltage follower circuit. The drop-synchronizer is functioned by the control of the computer. The alternating current potential which is superposed on the direct potential is 15 mV and its frequency is adjusted to 34.5 Hz.

**Computer.** The analog to digital converter samples the polarographic current in 8-bit digital data every 240  $\mu$  sec. At the start, the mercury drop is knocked off with a pulse provided by the computer. The computer waits 3.5 sec for the growth of the mercury drop and begins to sample the polarographic current. It samples 121 points during a period of the applied AC potential and continues to sample until 16 sets of digital data in total are obtained.

**Synchroscope.** The synchroscope controls the gate of the computer, *i.e.*, it sends a triggering pulse to the computer so that the computer can start sampling at the time when the phase angle of the applied AC potential becomes zero. At the end of the period of the applied AC potential, the computer stops sampling, waits for the next triggering pulse from the synchroscope and again begins to sample the polarographic current. Sampling by the computer is performed during every period of the applied AC potential with the aid of the control of the synchroscope. The AC voltage which is sent to the synchroscope as the triggering source has to be large enough to achieve stability of triggering level.

**Measurements.** A reversible system of Cd(II) ion in

- 1) D. E. Smith, *Anal. Chem.*, **35**, 602 (1963).
- 2) D. E. Smith, *ibid.*, **35**, 610 (1963).
- 3) T. G. McCord, E. R. Brown, and D. E. Smith, *ibid.*, **38**, 1615 (1966).
- 4) T. G. McCord and D. E. Smith, *ibid.*, **40**, 289 (1968).
- 5) T. G. McCord and D. E. Smith, *ibid.*, **41**, 1423 (1969).
- 6) T. G. McCord and D. E. Smith, *ibid.*, **42**, 2 (1970).
- 7) T. G. McCord and D. E. Smith, *ibid.*, **42**, 126 (1970).

- 8) T. Kugo, Y. Umezawa, and S. Fujiwara, *Chem. Instrument.*, **2(2)**, 189 (1969).

- 9) Model JRA-5 Spectrum Computer of Japan Electron Optics Laboratory Co.

- 10) Type 585 Cathode-Ray Oscilloscope of Tektronix, Inc.

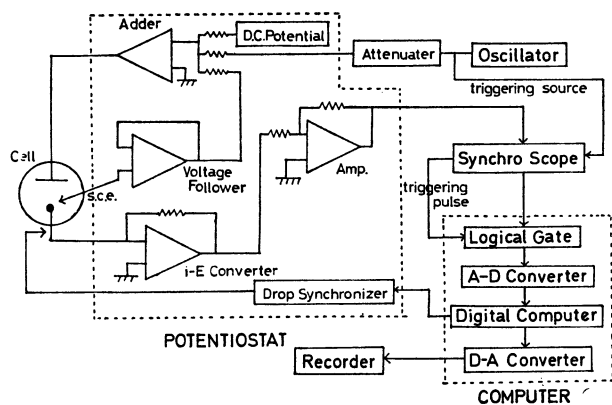


Fig. 1. Blockdiagram of the apparatus.

1.0 mol/l  $\text{Na}_2\text{SO}_4$  was used. Before the measurements, the triggering level of the synchroscope is adjusted by inserting a standard resistor (1.00 k $\Omega$ ) in place of the cell. The standard resistor is also employed in order to calibrate the frequency of the oscillator and the intensities of the Fourier spectra. Charging currents are measured with the use of a reference solution which does not contain a depolarizer. The cell resistance is measured to be 102  $\Omega$  at potentials where the faradaic current is negligible. All these measurements are carried out by the phase-selective detection involving the Fourier transformation. The flow rate of mercury is 1.44 mg/sec at mercury column height of 60 cm. The drop time is 5.8 sec at 0 V *vs.* SCE. All polarographic measurements are made at  $22.5 \pm 0.5^\circ\text{C}$ .

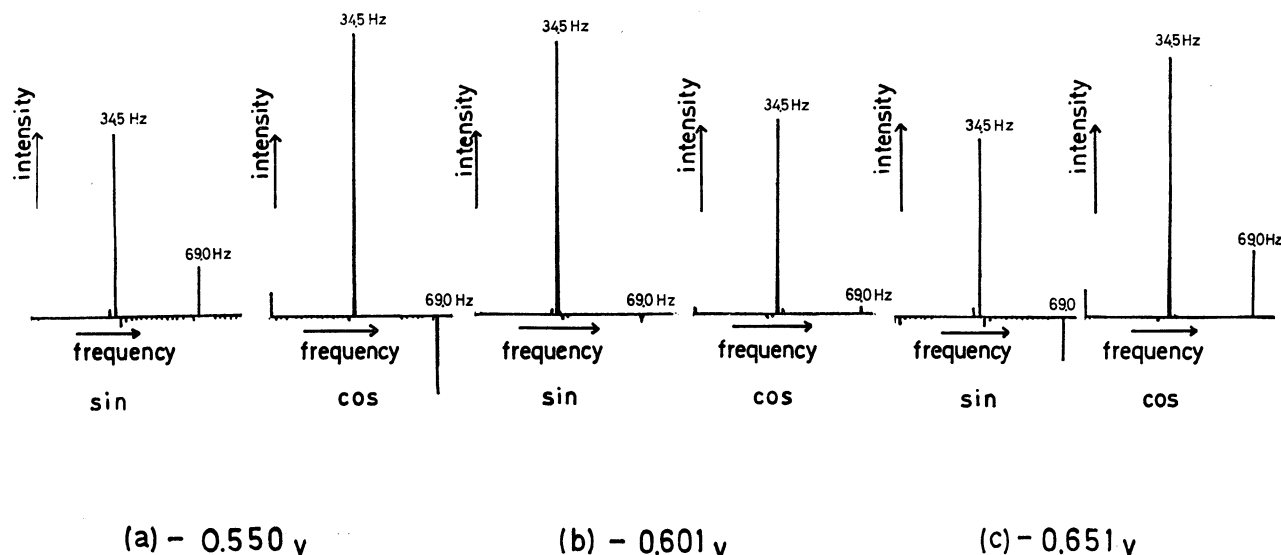
## Results and Discussion

*Fourier spectra of the Cd(II) System.* Figure 2 shows Fourier spectra for the Cd(II) system at three

potentials near the half-wave potential. The Fourier spectra are given at an interval of 2.15 Hz which is one sixteenth of the frequency of the applied AC potential. The 16th and the 32nd components correspond to the fundamental and the second harmonic AC polarographic waves, respectively. The sine part of the Fourier spectra corresponds to the component *in-phase* with the applied AC potential, whereas the cosine part represents the component which advances in phase by  $90^\circ$  relative to the AC potential.

Smith and Reinmuth<sup>11</sup> showed theoretically that in reversible electrode processes the phase angle of the fundamental harmonic AC polarographic wave is  $45^\circ$  at any DC potential, but the phase angle of the second harmonic AC wave<sup>12</sup> is  $135^\circ$  ( $-45^\circ$ ) at potentials more anodic (cathodic) than the half-wave potential. However, the Fourier spectra given in Fig. 2 are quite different in shape from this theoretical prediction. This result may be interpreted in terms of non-faradaic effects due to the double layer capacitance and the ohmic resistance of the system. The cosine part of the fundamental harmonic AC waves is larger in magnitude than the sine part (Figs. 2-a and 2-c). At  $-0.550$  V or  $-0.651$  V, the faradaic current is small, and the charging current becomes dominant. At  $-0.601$  V which is approximately equal to the half-wave potential, the sine part of the fundamental harmonic AC wave is dominant (Fig. 2-b). In the vicinity of the half-wave potential, the faradaic current is large enough to result in a considerable amount of IR-drop.

The second harmonic-AC wave is inverted in phase angle across the half-wave potential, where the second harmonic AC wave disappears. The intensity of the second harmonic AC waves given in Fig. 2 is much

Fig. 2. Fourier spectra of Cd(II) system at (a)  $-0.550$  V (b)  $-0.601$  V and (c)  $-0.651$  V.

System: 1.0 mM  $\text{CdCl}_2$  in 1.0 M  $\text{Na}_2\text{SO}_4$ .

AC potential: 34.5 Hz, 30 mV peak-to-peak sine wave.

Measurement: instantaneous AC polarographic current during 3.5–5.0 sec of drop life.

Spectrum: each Fourier component is given at an interval of 2.15 Hz and the intensity is arbitrarily scaled.

11) D. E. Smith and W. H. Reinmuth, *Anal. Chem.*, **33**, 482 (1961).

12) The phase angle of the second harmonic AC wave is taken so that the sign of the amplitude can be positive.

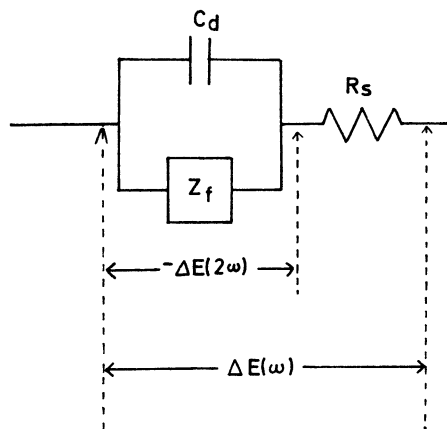


Fig. 3. Equivalent circuit to the cell.  
 $\Delta E(\omega)$  is the applied AC potential.  
 $\Delta E(2\omega)$  is the potential produced by the second harmonic alternating current.

smaller than what is predicted from the theory developed by Smith.<sup>11)</sup> This discrepancy may be interpreted in terms of the IR-drop of the system as follows. The circuit which is equivalent to the cell is shown in Fig. 3, where  $Z_f$ ,  $C_d$ , and  $R_s$  denote the faradaic impedance, the double layer capacitance and the cell resistance respectively. When an AC potential whose angular frequency is  $\omega$  is applied to the electrode, and an additional AC potential with  $2\omega$  is also produced onto  $Z_f$  and  $C_d$ . This is because the second harmonic alternating current passes through  $R_s$ . The additional AC potential which is represented by  $-\Delta E(2\omega)$  in Fig. 3 produces a fundamental harmonic AC wave with  $2\omega$ , which is opposite in phase to the second harmonic AC wave produced by the applied AC potential with  $\omega$ . This leads to an appreciable decrease in the intensity of the second harmonic AC wave.<sup>13)</sup>

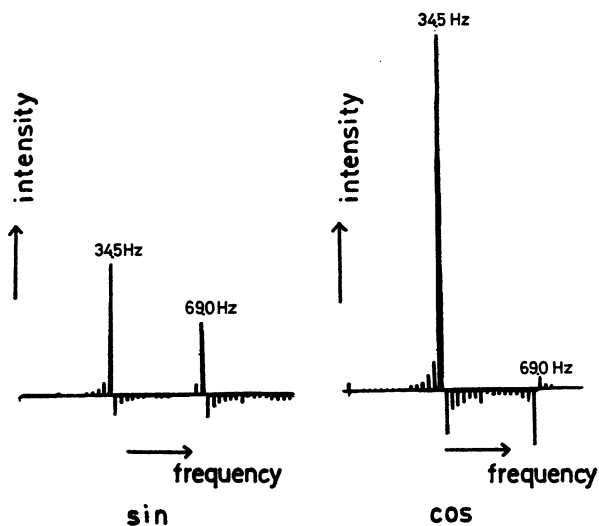


Fig. 4. Fourier spectrum of Cd(II) at  $-0.550$  V.  
 The polarographic current is sampled consecutively during 16 periods of the applied AC potential without the aid of triggering pulses.

13) The double layer capacitance  $C_d$  also reduces the second harmonic AC wave a little.

In addition to the fundamental and the second harmonic AC waves mentioned above, a number of small peaks are observed in Fig. 2. Possible origins for these small peaks are the growth of the dropping mercury electrode and instability of the oscillator.

It can be shown that the growth of the mercury drop results in the additional small peaks, which become smaller in intensity as the frequencies of the small peaks are separated from those of the main components. It can also be shown that the drop growth makes only a minor contribution to the intensity of the main components. Details of the calculation are given in Appendix II.

Instability of the oscillator can effectively be compensated by the aid of a triggering pulse supplied by the synchroscope, which controls the start of sampling for every period of the applied AC potential. Sharp spectra such as shown in Fig. 2 can only be obtained under this control. Figure 4 shows an example obtained in the absence of the control of the synchroscope. We see that the intensity, and therefore the number of small peaks, is increased remarkably. Such spectra cannot be used to analyze faradaic components quantitatively.

*Comparisons with the Calculated Curves.* The current amplitude-DC potential curves are illustrated in Figs. 5 and 7 for the fundamental and the second harmonic AC polarographic waves, respectively.<sup>14)</sup> The phase angle-DC potential curves are plotted in Figs. 6 and 8. In Figs. 5—8, solid lines show the

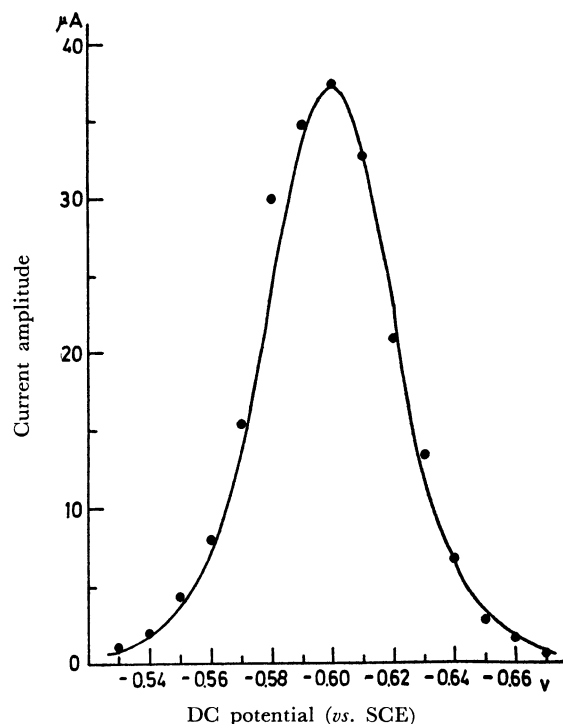


Fig. 5. Current amplitude-DC potential curve for the fundamental harmonic AC polarographic wave of the Cd(II) system.

(•••): experimental, (—): calculated

14) Fourier spectra are measured every 10 mV in the range from  $-0.530$  V to  $-0.660$  V and the contribution from the non-faradaic effects is eliminated.

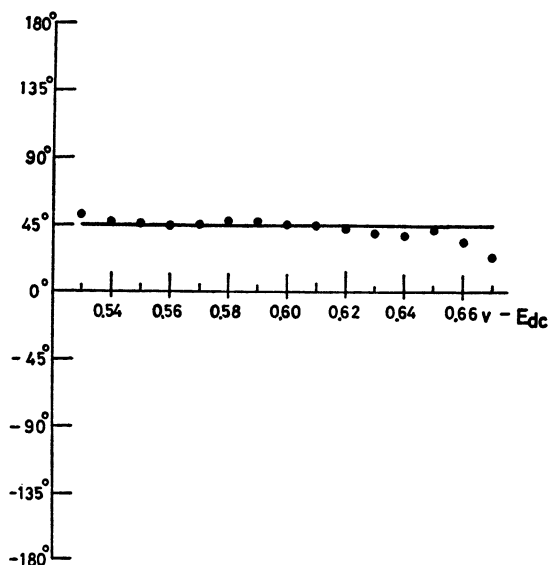


Fig. 6. Phase angle-DC potential curve for the fundamental harmonic AC polarographic wave of the Cd(II) system. (•••): experimental, (—): calculated

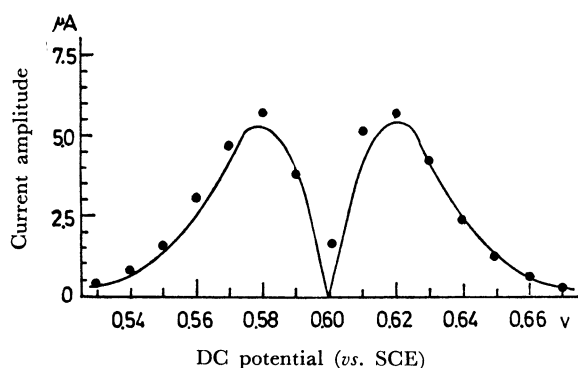


Fig. 7. Current amplitude-DC potential curve for the second harmonic AC polarographic wave of the Cd(II) system. (•••): experimental, (—): calculated

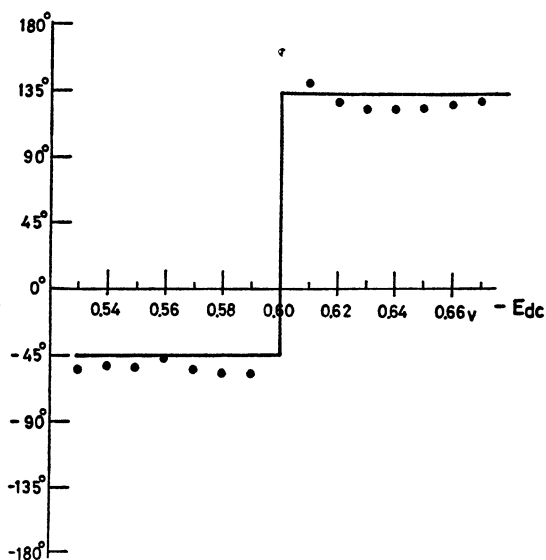


Fig. 8. Phase angle-DC potential curve for the second harmonic AC polarographic wave of the Cd(II) system.

theoretical curves obtained as in the following; the theoretical curves of the fundamental and the second harmonic-AC polarographic waves with the reversible process have been given by McCord and Smith<sup>4)</sup> as

$$I(\omega t) = \frac{n^2 F^2 A C_0^* (\omega D_0)^{1/2} \Delta E}{4 R T \cosh^2(j/2)} \sin(\omega t + \pi/4) \quad (4)$$

$$I(2\omega t) = \frac{n^3 F^3 A C_0^* (2\omega D_0)^{1/2} \Delta E^2 \sinh(j/2)}{(4 R T)^2 \cosh^3(j/2)} \times \sin(2\omega t - \pi/4) \quad (5)$$

$$j = \frac{nF}{RT} (E_{dc} - E_{1/2}^r) \quad (6)$$

where  $I(\omega t)$  and  $I(2\omega t)$  represent the fundamental and the second harmonic AC waves, respectively. Other notations are defined in Appendix I. In calculating  $I(\omega t)$  and  $I(2\omega t)$ , the value of  $nFAC_0^*D_0^{1/2}$  was obtained using Eq. (7) along with the intensity of the diffusion-controlled DC polarographic wave,<sup>15)</sup>

$$I_d(t) = \sqrt{\frac{7}{3}} nFAC_0^* D_0^{1/2} \frac{1}{\sqrt{\pi t}}. \quad (7)$$

As Figs. 5—7 show the experimental plots are in good agreement with the calculated curves. In Fig. 8 a considerable deviation is noticed in the case of the phase angle of the second harmonic AC wave. This is because Eq. (5) for the second harmonic AC wave is valid only for the ideally reversible process. The Cd(II) system which is not ideally reversible has a *quasi-reversibility* in the fundamental harmonic AC process. McCord and Smith have taken the effect of the *quasi-reversibility* into account, and given more precise equations.<sup>4)</sup> The results given in Fig. 8 can satisfactorily be reproduced using these equations. As discussed by McCord and Smith, the phase angle of the second harmonic AC wave is influenced by the *quasi-reversibility* of the electrode reaction more sensitively than that of the fundamental harmonic AC wave.

#### General Characteristics of the Fourier Analysis.

Figure 9 illustrates the charging current and its Fourier spectrum for a 1.0 mol/l Na<sub>2</sub>SO<sub>4</sub> solution at -0.601 V. It should be noted that the charging current in-

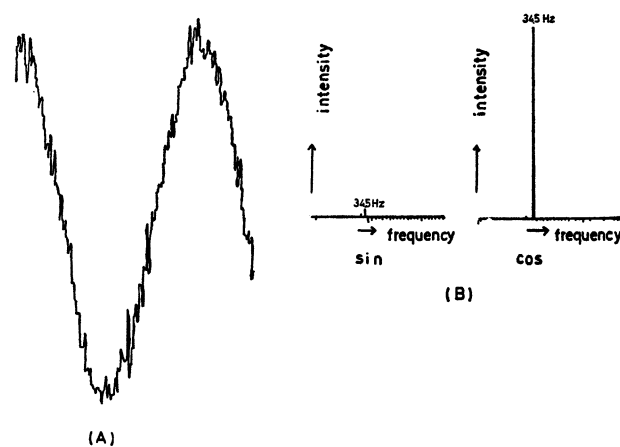


Fig. 9. Charging current and its Fourier spectrum of 1.0 M Na<sub>2</sub>SO<sub>4</sub> solution at -0.601 V.

15) P. Delahay, "New Instrumental Methods in Electrochemistry," Interscience, New York (1954), p. 63.

volving much noise reproduces the Fourier spectrum satisfactorily. This is closely related to the process of numerical integration in the Fourier analysis; a possible contribution from noise is cancelled if the number of sampling points is large enough compared to the inverse of an average frequency of the noise. In this respect the results in Figs. 5—9 are not quite satisfactory. A computer with larger memory capacity and an analog to digital converter with higher resolution and speed would consolidate the advantage of the present method of Fourier analysis. *Accumulation* of signals would also serve for an improvement of the results.

In the analysis of electrode reactions, the second harmonic AC polarographic wave is more useful than the fundamental harmonic AC wave. In the first place, the former is not affected by the non-faradaic effects; the IR-drop of the system can be compensated properly by the application of the *positive feed back technique* in the potentiostat.<sup>16-18)</sup> In contrast, when using the fundamental harmonic AC wave, it is difficult to eliminate accurately the effects of the double layer capacitance. Secondly, the line shape of the second harmonic AC wave responds more sensitively to the electrode reaction kinetics. As suggested by McCord and Smith,<sup>4)</sup> the current amplitude-DC potential curve and the phase angle-DC potential curve are useful in analyzing the reaction scheme at the electrode.

In spite of these advantages, the second harmonic AC wave has seldom been used. This is because it is difficult to measure the second harmonic AC wave accurately for lack of sensitivity. The phase angle of the second harmonic AC wave in particular seems to have never been measured. In view of the above discussion, the method of the Fourier Transformation given here seems promising for an accurate analysis of the second harmonic AC wave.

The authors are indebted to Drs. Yoji Arata and Takeo Yamamoto for their valuable advice. They are also grateful to Mr. Teruhiko Kugo of Yanagimoto Manufacturing Co. for his helpful suggestions on measurements.

16) E. R. Brown, T. G. McCord, D. E. Smith, and D. D. Deford, *Anal. Chem.*, **38**, 1119 (1966).

17) E. R. Brown and D. E. Smith, *ibid.*, **40**, 1411 (1968).

18) E. R. Brown, H. L. Hung, T. G. McCord, D. E. Smith, G. L. Booman, *ibid.*, **40**, 1420 (1968).

## Appendix

### I. Notations

- $A$  = electrode area
- $C_0^*$  = initial concentration of oxidized form
- $E_{dc}$  = DC component of applied potential
- $\Delta E$  = amplitude of applied alternating current potential
- $E_{1/2}^r$  = reversible polarographic half-wave potential
- $F$  = Faraday's constant
- $R$  = gas constant
- $T$  = absolute temperature
- $n$  = number of electrons transferred in heterogeneous charge transfer step
- $I_d(t)$  = instantaneous DC faradaic limiting current
- $I_{\omega}(t)$  = fundamental harmonic faradaic alternating current
- $I(2\omega t)$  = second harmonic faradaic alternating current
- $\omega$  = applied angular frequency
- $s$  = rate of increase in amplitude of polarographic alternating current
- $t$  = time

### II. Effect of the Drop Growth upon Fourier Spectra.

Equation (1) should be modified in order to take into account the effect of the drop growth. It is a good approximation that the amplitude of the AC polarographic current changes almost linearly. Using the rate  $s$  of the increase in the amplitude the AC polarographic wave can be represented by the equation

$$I = \sum_{k=1}^{\infty} (1+st) I_k \sin(k\omega t + \varphi_k), \quad (A1)$$

where  $k$  denotes the order of each harmonic AC component. Eq. (A1) is expanded into the Fourier series in the range  $0 \leq t \leq T$ ,

$$\begin{aligned} I = & \sum_{k=1}^{\infty} I_k \left\{ \cos \varphi_k \left( 1 - \frac{s}{2\omega k} \right) \sin k\omega t \right. \\ & + \sin \varphi_k \left( 1 - \frac{s}{2\omega k} \right) \cos k\omega t \\ & + \frac{sT \cos \varphi_k}{2\pi} \sum_{\substack{n=0 \\ n \neq km}}^{\infty} \frac{-2km}{k^2 m^2 - n^2} \cos n \frac{\omega}{m} t \\ & \left. + \frac{sT \sin \varphi_k}{2\pi} \sum_{\substack{n=1 \\ n \neq km}}^{\infty} \frac{2n}{k^2 m^2 - n^2} \sin n \frac{\omega}{m} t \right\}, \quad (A2) \end{aligned}$$

where  $m$  represents  $\omega T/(2\pi)$ , i.e., the number of periods of the fundamental harmonic AC components in  $T$ . Equation (A2) shows that the intensity of each main component of the Fourier spectra is reduced by  $s/(2\omega k)$ . Under the present experimental conditions, viz.,  $\omega = 216.7$  and  $s < 2$ , the value of  $s/(2\omega k)$  is less than 0.005 for each order harmonic AC component. Equation (A2) can also describe the behavior of small peaks beside each main component.